Science and Engineering Research Council

Rutherford Appleton Laboratory

Chilton DIDCOT Oxon OX11 0QX   RAL-93-075

On the Local Constitutive and Directed Graph Network Representations of Response Factors

MATH
ERSU
ENG
BLDG

A D Irving S Dudek G Warren and T Dewson

October 1993

On the local constitutive and directed graph network representations of response factors

A D Irving+, S J M Dudek[o], G Warren[o] and T Dewson*

+ Rutherford Appleton Laboratory, Chilton, Oxford, Oxon, OX11 0QX, UK.

[o] Department of Building Science, The University, Newcastle Upon Tyne, NE1 7RU, UK.

* Department of Mathematics, University Walk, University of Bristol, Bristol, BS8 1TR, UK.

Abstract

Many of the calculation procedures for determining the thermal transport through building walls are based on thermostat directed graph networks. These procedures relate the heat flux and temperature in one region of the wall to the heat flux and temperature in another region of the wall. Recently an ASHRAE sponsored project examined the ability of such procedures to correctly predict the performance of a number of wall types. That study showed indicated that the design calculations were only accurate to the 50% level.

A thermal transport processes can be represented in either a local constitutive convolution form or as a directed graph network form. Both the local constitutive convolution and network representations are based on response factors which can, in principle, be used to estimate dynamic thermal transmission of the building components.

The purpose of this paper is to show that only the local constitutive equations yield, for all cases, consistent and accurate values for the physical properties of the materials under test, whereas the directed graph network representations are unreliable. This is because the network representations are ill posed and are likely to lead to erroneous predictions in designing the performance of buildings. The constitutive representation allows the measurement of thermal conductivity and transmission of building components under real meteorological conditions. It is then used to measure the convective and radiative coefficients of a wall and the representation can be extended to the nonlinear thermal transport case.

Introduction

An observed thermodynamic flux can be characterised in terms of the observed thermodynamic forces with the constants of proportionality being the transport coefficients. Mitalas and Stephenson [1,2] have applied the response factor form of the directed graph network approach to the characterisation of thermal flow in buildings. Their method is used in heating and cooling load calculations for design [3]; however it has proved difficult to extract accurate and consistent response values from experimental data [4]. In order to assess the impact of a particular construction on energy transport, information about the thermal transport processes and their thermodynamic properties interactions with the thermodynamic properties is essential. Thus this paper presents a constitutive convolution form that provides information on the thermodynamic interactions.

The most simple case to examine is the one dimensional thermal conduction in a solid body. A thermal transport processes can be represented in either a local constitutive convolution form or as a directed graph network form. Both the local constitutive convolution and directed graph network representations are based on response factors which can, in principle, be used to estimate dynamic thermal transmission of the building components. The thermal conductivity of the solid is estimated using each of the representations and these estimated values are then used to test the ability of each representation to predict the future behaviour of the building. The response factors can be estimated directly from the time series data of the physical observables under general stochastic boundary conditions.

The first part of this paper examines the ability of the constitutive and directed graph network representations to accurately characterise and to predict the thermal performance of a well defined thermal transport problem. Of these, only the constitutive convolution equation representation based on the response factors was consistently able to determine accurate values for the thermal conductivity of a wide range of building materials. The second part of this paper considers the simultaneous extraction of the conductive, convective and radiative thermal transport coefficients from building performance time series data.

A specially constructed test facility was used to measure the thermal conductivity of a wide range of common building materials. The thermal conductivity of each material being determined under dynamical meteorological boundary conditions. The time series data were analysed by two representations and compared to the ratio of mean's method and to available published data. The actual duration of data collection being chosen to be greater that three times the relaxation time of the thermal conduction process, and the number of time series data points being sufficient to perform a detailed analysis, typically several hundred points.

Representations of the thermal process

The representations for thermal transport used in this work are:

1. the directed graph network representation, where the heat flux and temperature in one region of the solid is related to the historical heat flux and temperature in another region.

2. the local constitutive representation where the one dimensional heat flux in the solid material is assumed to be related to the historical temperature gradients.

The moment hierarchy method [5] is used to calculated the coefficients for each of these representations.

Directed graph networks

One way to characterise the relationship between subsystems within the thermodynamic environment by analogy with electrical multiport networks. The most simple directed graph network case to examine is the relationship between the heat flux and the temperature field measured on each side of a plane parallel slab, which can be regarded as a vector constitutive problem. Carslaw and Jaeger [6] first considered the relationship between the heat flux, $\{Q_k(t)\}$, and the temperature values, $\{T(t)\}$, on each surface of a parallel sided homogeneous isotropic slab to be a matrix algebra problem in the z domain.

Mitalas and Stephenson [1] have extensively applied the response factor form of the directed graph network approach to characterise the one dimensional thermal conduction problem in the building envelope, in the z domain their representation is given by

$$
\begin{vmatrix} \Theta_1(z) \\ \Phi_1(z) \end{vmatrix} = \begin{vmatrix} A_{\Theta_1\Theta_2}(z) & B_{\Theta_1\Phi_2}(z) \\ C_{\Phi_1\Theta_2}(z) & D_{\Phi_1\Phi_2}(z) \end{vmatrix} \begin{vmatrix} \Theta_2(z) \\ \Phi_2(z) \end{vmatrix}
\tag{1}
$$

where $\Theta_1(z)$ and $\Theta_2(z)$ are the z transformations of the heat fluxes, where $\Phi_1(z)$ and $\Phi_2(z)$ are the z transformations of the temperatures and where $A_{\Theta_1\Theta_2}(z)$, $B_{\Theta_1\Phi_2}(z)$, $C_{\Phi_1\Theta_2}(z)$ and $D_{\Phi_1\Phi_2}(z)$ are the z transformations of the time domain response factors in equation (1).

In the time domain the observed thermal heat flux in terms of the temperature field with linear directed graph network expressions to describe the relationships between the heat fluxes and temperature fields with the vector convolution

$$
\begin{vmatrix} Q_1(t) \\ T_1(t) \end{vmatrix} = \begin{vmatrix} K_{Q_1Q_2}(\sigma) & K_{Q_1T_2}(\sigma) \\ K_{T_1Q_2}(\sigma) & K_{T_1T_2}(\sigma) \end{vmatrix} \begin{vmatrix} Q_2(t-\sigma) \\ T_2(t-\sigma) \end{vmatrix}
\tag{2}
$$

where $K(\sigma)$'s are the response factors of the process, where σ is the time delay with respect to the present time t, and where the time delays are assumed to extend to the finite memory μ for the conduction process.

Local constitutive relationship

A thermodynamic system which is embedded in an open environment experiences a set of thermodynamic potentials, whose gradients, called the thermodynamic forces, $\{F_i(t)\}$, cause the exchange of certain properties, called the thermodynamic fluxes, $\{Q_k(t)\}$ between the system and the environment.

4

Each local thermodynamic flux, $\{Q_k(t)\}$, is characterised in terms of the observed thermodynamic forces, $\{F_i(t)\}$; for example conduction, convection and radiation, with

$$Q_k(t) = Q_k(F_1,...,F_A) \qquad (3)$$

Onsager related the linear steady state irreversible thermodynamic fluxes to the local linear steady state thermodynamic forces which motivate the flux [7,8]. The linear constitutive equations relate the independent thermodynamic fluxes, $\{Q_k(t)\}$, in terms of their conjugate thermodynamic forces, $\{F_i(t)\}$, and a set of linear steady state Onsager coefficients, L_{ik}, with

$$Q_k(t) = \sum_i L_{ik}F_i(t) \qquad (4)$$

and where the linear steady state transport coefficients are given by $L_{ik} = \left(\dfrac{\partial Q_k}{\partial F_i}\right)_0$

The Onsager representation considered here are concerned with the constitutive equations whose constants of proportionality are the transport coefficients.

The most simple case to study is the one dimensional heat conduction experiment. Gurtin and Pipkin [9] developed a realistic field theory for heat conduction using constitutive equations with assumptions that lead to finite propagation speeds. The linearised constitutive equation for the heat flux in terms of the local temperature gradient being

$$Q_k(t) = \sum_{\sigma=0}^{t} L_{Q_k\nabla T}(t-\sigma)\nabla T(\sigma) \qquad (5)$$

where the linear thermodynamic force is equal to the temperature gradient, i.e. $F_i(t) = \nabla T(t)$. Chen and Nunziato [10] used the second law of thermodynamics to show that

$$\kappa = \sum_{\sigma=0}^{t} L_{Q_k\nabla T}(\sigma) > 0 \qquad (6)$$

where κ is the steady state thermal conductivity of the solid.

Ratio of Means Method

In addition to the two time series representations given above the thermal conductivity of the sample materials will estimated using the ratio of means method and also from the literature. In the ratio of means method steady state conditions are assumed to prevail and the relationship between the local heat flux and the local temperature gradient will be given by the approximation

$$\sum_{t=1}^{N} Q_k(t) \approx -\kappa_3 \left(\sum_{t=1}^{N} T_2(t) - \sum_{t=1}^{N} T_1(t) \right) \tag{7}$$

where N is the sample length, where it has been assumed that the thickness $\Delta x = 1.0$ and where the conductivity from the ratio of means method, κ_3, is

$$\kappa_3 \approx \frac{\sum_{t=1}^{N} Q_k(t)}{\left(\sum_{t=1}^{N} T_2(t) - \sum_{t=1}^{N} T_1(t) \right)} \tag{8}$$

where it is implicit that the heat flux and temperature values are measured in steady state and that the temperature difference used is the actual driving force of the heat flux.

6

Response factor estimation for the directed graph network approach

An ordered sequence of data in time is called a time series and the relationship between series sequences can be characterised in terms of response factor values. In the thermostatic representation it is assumed that the heat flux, $\{Q_1(t)\}$, and temperature field, $\{T_1(t)\}$, measured in one local thermodynamic region are a linear vector function of the heat flux, $\{Q_2(t)\}$, and temperature field, $\{T_2(t)\}$, in another region. The network equation for the time domain form of the Mitalas and Stephenson directed graph representation is given by

$$\begin{vmatrix} Q_1(t) \\ T_1(t) \end{vmatrix} = \begin{vmatrix} K_{Q_1 Q_2}(\sigma_1) & K_{Q_1 T_2}(\sigma_1) \\ K_{T_1 Q_2}(\sigma_1) & K_{T_1 T_2}(\sigma_1) \end{vmatrix} \begin{vmatrix} Q_2(t-\sigma_1) \\ T_2(t-\sigma_1) \end{vmatrix} \tag{9}$$

The equation for the heat flux is explicitly given by the convolution

$$Q_1(t) = \sum_{\sigma_1=0}^{\mu} K_{Q_1 Q_2}(\sigma_1) Q_2(t-\sigma_1) + \sum_{\sigma_1=0}^{\mu} K_{Q_1 T_2}(\sigma_1) T_2(t-\sigma_1) \tag{10}$$

and the steady state thermal conductivity and heat flux gain, κ_1 and ψ_1, for the network representation will be given by

$$\kappa_1 = \sum_{\sigma_1=0}^{\mu} K_{Q_1 T_2}(\sigma_1) \quad \text{and} \quad \psi_1 = \sum_{\sigma_1=0}^{\mu} K_{Q_1 Q_2}(\sigma_1) \tag{11}$$

That is, the area under the response factor between the local heat flux and local temperature gradient is equal to the steady state thermal conductivity; where it has been assumed that $\Delta x = 1$. More generally, the area represents the steady state gain between physical observables [5].

A set of $2(\mu+1)$ equations need to be generated and solved for the response factor values, $K_{Q_1T_2}(\sigma_1)$. If the temperature fields, $\{T_1(t)\}$ and $\{T_2(t)\}$, and heat fluxes, $\{Q_1(t)\}$ and $\{Q_2(t)\}$ are drawn from stochastic processes, then the moment equations are

$$M_{T_2Q_1}(\tau_1) = \sum_{\sigma_1=0}^{\mu} K_{Q_1Q_2}(\sigma_1) M_{T_2Q_2}(\tau_1,\sigma_1) + \sum_{\sigma_1=0}^{\mu} K_{Q_1T_2}(\sigma_1) M_{T_2T_2}(\tau_1,\sigma_1) \qquad (12)$$

and

$$M_{Q_2Q_1}(\tau_1) = \sum_{\sigma_1=0}^{\mu} K_{Q_1Q_2}(\sigma_1) M_{Q_2Q_2}(\tau_1,\sigma_1) + \sum_{\sigma_1=0}^{\mu} K_{Q_1T_2}(\sigma_1) M_{Q_2T_2}(\tau_1,\sigma_1) \qquad (13)$$

where the moments represent the average values of delayed products.

For example the cross moments $M_{T_2Q_1}(\tau_1) = \sum_{t=0}^{N} T_2(t-\tau_1) Q_1(t)$ and

$M_{Q_2T_2}(\tau_1,\sigma_1) = \sum_{t=0}^{N} Q_2(t-\tau_1) T_2(t-\sigma_1)$, where N is the length of the data sample. Equation (12) can be seen to be a linear algebra expression $\underline{c} = \underline{\underline{a}}\underline{h}$, where $\underline{\underline{a}}$ is the auto moment matrix, $\underline{c}$ is the cross moment vector and $\underline{h}$ is the vector of response factor values [5].

Response factor estimation for the local constitutive approach

The local constitutive representation is a field theoretical one in which the one dimensional heat conduction in an isotropic solid which contains no sources of heat. It is assumed that the heat flux observed can be expressed as a convolution between the observed heat flux, $Q_k(t)$, and the local temperature gradient, $\nabla T(t)$, and the linear temporal response factor, $L_{Q_k \nabla T}(\sigma_1)$. For a discrete process which possesses a finite memory of duration μ, the convolution can be expressed as

$$Q_k(t) = \sum_{\sigma_1=0}^{\mu} L_{Q_k \nabla T}(\sigma_1) \nabla T(t-\sigma_1) \qquad (14)$$

where σ_1 denotes lag and where μ is the finite memory of the conductive process.

8

The response factor, $L_{Q_k \nabla T}(\sigma_1)$, is related to the steady state thermal conductivity, κ_2, [10]

with

$$\kappa_2 = \sum_{\sigma_1=0}^{\mu} L_{Q_k \nabla T}(\sigma_1) \qquad (15)$$

A tractable moment hierarchy comprising of a set of $(\mu+1)$ equations with well behaved coefficients is obtained which can be solved for the response factor values, $L_{Q_k \nabla T}(\sigma_1)$, with

$$M_{\nabla T Q_k}(\tau_1) = \sum_{\sigma_1=0}^{\mu} L_{Q_k \nabla T}(\sigma_1) \, M_{\nabla T \nabla T}(\tau_1, \sigma_1) \qquad (16)$$

where $M_{\nabla T Q_k}(\tau_1)$ and $M_{\nabla T \nabla T}(\tau_1, \sigma_1)$ are the cross and auto moments.

Experimental facility for the thermal conductivity experiment

The experimental arrangement shown in figure 1 was designed to measure the thermal conductivity of a wide range of medium to low thermal conductivity engineering materials under stochastic boundary conditions. Different sized samples were required to measure the thermal conductivity, the dimensions for each material type were determined using a two dimensional finite element model was used. This allowed rapid optimisation of sample size and establishing the best positions of the sensors.

Essentially the rig consists of a heat pipe to atmospheric conditions and another heat pipe to a cold temperature bath which is controlled. The cold bath is an enclosed copper heat exchanger that has cold water pumped through it. The cooling of the water is achieved by using a commercial water chiller. The water is re-circulated through the chiller. The water temperature is fixed at 10.0+/- 0.02°C.

9

The temperature and heat flux are measured at positions above and below the as shown in figure 1. The test section is surrounded by loose vermiculite insulation. The insulation is contained within a 500 mm square box.

The readings are taken every ten seconds over an eleven hour period, the time interval for data collection being determined by the response time of the sensors used. During the test period 4,000 sets of measurements are taken. Of these 4000 points, some 2000 are used to estimate the response factor values of the process and the remaining 2000 points are used to compare with the values of the heat flux predicted using the estimated response factor values.

Analysis of the data

The thermal conductivity of each sample was determined using the two representations and the ratio of means method. These estimated values are then used to predict the future behaviour of the heat flux at the surface of the sample. These predicted heat flux values are then compared with the actual observed values.

The conductivity values estimated using the local constitutive and the Mitalas and Stephenson directed graph network representations are compared with the values obtained using the ratio of means method and where appropriate from the literature.

The estimated response factor values obtained using the time series techniques can then be used to provide a prediction of the local heat flux , $\{Q_p(t)\}$, field which may be compared with the measured heat flux, $\{Q_1(t)\}$. This provides a quantitative measure of the quality of the response factor characterisation of the thermal transport process, both for the region of data which were used to estimate the response factor values and for regions of the data that were not used in the response factor estimation process. The accuracy of the modelling ability was determined by comparing the root mean square and also the Students t-test between the actual, $\{Q_1(t)\}$, and predicted, $\{Q_p(t)\}$, time series sequences. These estimated response function values are used to predict the future behaviour of the material, with the accuracy of the predictive ability being determined by comparing the root mean square and also the Students t-test between the actual, $\{Q_1(t)\}$ which were not used to estimate the transport coefficients, and predicted, $\{Q_p(t)\}$, time series sequences. This provides a sensitive measure of the quality of the response factor characterisation of the thermal transport process, both for the region of data which were used to estimate the response factor values and for other data sets which were not used in the estimation process.

In all cases the values of the test statistics for the differences between the measured, $\{Q_1(t)\}$, and predicted, $\{Q_p(t)\}$, output heat flux for both modelled and predicted data lay well within the acceptance region; thus each representation can accurately characterise the observed behaviour of the heat flux.

11

At this stage the representations are only black-box characterisations, and none of them can be rejected on the basis of the findings of the analysis.

The important thing is to determine if the coefficient values have any physical meaning. In this case, if the coefficient values are related to the thermal conductivity of the material. In addition, the robust and consistent nature of the coefficients needs to be established.

The values of the estimated thermal transport conductivities are presented in table 1. The experimental uncertainties given are dominated by the calibration accuracy of the heat flux mats.

Table 1: Estimated thermal conductivities of a range of materials

	directed graph network		local constitutive	ratio of means	Literature value
	κ_1 W /m °K	ψ_1 flux gain	κ_2 W /m °K	κ_3 W /m °K	
marble	2.78 ±0.40	-0.68 ±0.22	1.64 ±0.18	1.636 ±0.18	2.00 ±0.01
clay tile	0.616 ±0.35	-0.204 ±0.22	1.08 ±0.05	1.08 ±0.05	1.00 ±0.05
plaster board	0.295 ±0.03	0.586 ±0.04	0.200 ±0.01	0.199 ±0.01	0.17 ±0.01
cork	0.030 ±0.006	0.989 ±0.10	0.050 ±0.005	0.050 ±0.005	0.050 ±0.003

As can be seen the local constitutive representation gives correct, accurate and consistent values for the conductivities over the whole range of materials considered. In contrast the Mitalas and Stephenson representation fails to provide accurate or consistent values for the building materials considered here.

The reason that the Mitalas and Stephenson directed graph network representation is not consistent and fail to give the correct answers for the thermal transport coefficients can be seen from the basic formulation of the problem, in that it is assumed the functional relationship is of the form

$$Q_2(t) = f(Q_1, T_1, t)$$

As the heat flow is approximately one dimensional through the slab of material then $Q_2(t) \approx Q_1(t)$ and the equation is ill posed, as it can be written as

$$Q_2(t) \approx Q_1(t) + \delta \ (Q_1, T_1, t) \ .$$

In table 2 the estimated conductivity for different samples are given.

Table 2: Estimated thermal conductivities of different samples

	directed graph network		local constitutive	ratio of means	Literature value
	κ_1 W /m °K	ψ_1 flux gain	κ_2 W /m °K	κ_3 W /m °K	
clay tile 1	0.616 ±0.35	-0.204 ±0.22	1.08 ±0.05	1.08 ±0.05	1.00 ±0.05
 2	0.355 ±0.06	0.296 ±0.06	1.08 ±0.05	1.08 ±0.05	1.00 ±0.05
 3	0.188 ±0.05	0.611 ±0.10	1.08 ±0.05	1.06 ±0.05	1.00 ±0.05
 4	0.128 ±0.030	0.723 ±0.050	1.08 ±0.05	1.07 ±0.05	1.00 ±0.05
cork 1	0.030 ±0.006	0.989 ±0.10	0.050 ±0.005	0.050 ±0.005	0.050 ±0.003
 2	0.029 ±0.006	0.235 ±0.05	0.050 ±0.005	0.050 ±0.005	0.050 ±0.003
 3	-0.019 ±0.006	1.56 ±0.20	0.050 ±0.005	0.050 ±0.005	0.050 ±0.003
 4	0.021 ±0.006	0.488 ±0.10	0.050 ±0.005	0.050 ±0.005	0.050 ±0.003

Again the local constitutive representation gives results that are consistent and which agree within the error bars, but which are slightly low because of contact resistance effects. However, the Mitalas and Stephenson directed graph representation fails to provide consistent values for the building materials considered here because the representation is ill posed.

Current many of the thermal transport calculation procedures for buildings are based on the Mitalas and Stephenson directed graph representation.

This being the case, is it very likely that building designs based on them will not accurately represent of the true performance of the actual building, see for example [4] which shows large discrepancies between the measured and the modelled thermal performance of a wide range of building construction types.

Response factor estimation for a conductor with convective and radiative forces

The above has demonstrated that the local constitutive response factor representation provides a accurate characterisation of the thermal conduction process and physically meaningful transport coefficients. In general, more than one thermodynamic potential will be acting to cause thermodynamic flow and in those cases the local constitutive equations are of a vector form.

In the present section the vector form of the local constitutive equations are used to simultaneously determine the convective and radiative heat transfer coefficients of a building surface under forced convective conditions.

---

[1] The material in this section was originally presented at a CIB W60 working party meeting in Athens 1991 [13]. The working party recommended that the material be published in the open literature.

The heat flux may be expressed as a convolution between the observed thermodynamic forces and the thermal response factor. A useful starting point is to consider the local energy balance at a typical building surface in terms of a superposition of the contributions from each thermodynamics force

$$Q(t) = Q_{conduction}(t) + Q_{radiation}(t) + Q_{convection}(t) \qquad (17)$$

As for the one dimensional conduction equation given by (5), this can be written in terms of the linear convolution of the local thermodynamic forces and the response factors for each process with

$$
\begin{aligned}
Q(t) = &\sum_{\sigma_1=0}^{\mu} L_{Q\nabla T_s}(\sigma_1)\nabla T_s(t-\sigma_1) \\
&+ \sum_{\sigma_1=0}^{\mu} L_{Q\Delta T_r^4}(\sigma_1)\Delta T_r^4(t-\sigma_1) + \sum_{\sigma_1=0}^{\mu} L_{Q\Delta T_f}(\sigma_1)\Delta T_f(t-\sigma_1)
\end{aligned} \qquad (18)
$$

where μ is the finite memory of the transport process.

In this case the thermodynamic forces are:

1)   the conductive thermodynamic force is the temperature gradient $,\nabla T_s(\sigma_1)$ $^{\circ}K\,m^{-1}$, within the wall and the response factor values for the conductive process are $L_{Q\nabla T_s}(\sigma_1)$ $W\,^{\circ}K\,m^{-1}$

2)   the radiative thermodynamic force, $\Delta T_r^4(\sigma_1)$ $W\,m^{-2}$, is the Stefan-Boltzmann's constant multiplied by the difference between the fourth powers of the surface temperatures of the ceiling and the average of the remaining surfaces and the response factor values of the radiative process are $L_{Q\Delta T_r^4}(\sigma_1)$ and

3)   the convective thermodynamic force $,\Delta T_f(\sigma_1)$ $^{\circ}K$, is the temperature difference across the fluid-surface boundary layer , the response factor values of the convective process are $L_{Q\Delta T_f}(\sigma_1)$ $W\,^{\circ}K\,m^{-2}$.

The area under the estimated response factor $A=\sum_{\sigma=0}^{\mu} L_{QF}(\sigma_1)$ for a given thermodynamic force $F(t)$ for each process is the transport coefficient of that process.

16

The time series moment equations between the heat flux and the three thermodynamic forces are

a) the conductive moments

$$M_{\nabla T_s Q}(\tau_1) = \sum_{\sigma_1=0}^{\mu} L_{Q\nabla T_s}(\sigma_1) M_{\nabla T_s \nabla T_s}(\tau_1, \sigma_1)$$

$$+ \sum_{\sigma_1=0}^{\mu} L_{Q\Delta T_r^4}(\sigma_1) M_{\nabla T_s \Delta T_r^4}(\tau_1, \sigma_1) + \sum_{\sigma_1=0}^{\mu} L_{Q\Delta T_f}(\sigma_1) M_{\nabla T_s \Delta T_f}(\tau_1, \sigma_1)$$

(19)

b) the radiative moments

$$M_{\Delta T_r^4 Q}(\tau_1) = \sum_{\sigma_1=0}^{\mu} L_{Q\nabla T_s}(\sigma_1) M_{\Delta T_r^4 \nabla T_s}(\tau_1, \sigma_1)$$

$$+ \sum_{\sigma_1=0}^{\mu} L_{Q\Delta T_r^4}(\sigma_1) M_{\Delta T_r^4 \Delta T_r^4}(\tau_1, \sigma_1) + \sum_{\sigma_1=0}^{\mu} L_{Q\Delta T_f}(\sigma_1) M_{\Delta T_r^4 \Delta T_f}(\tau_1, \sigma_1)$$

(20)

and c) the convective moments

$$M_{\Delta T_f Q}(\tau_1) = \sum_{\sigma_1=0}^{\mu} L_{Q\nabla T_s}(\sigma_1) M_{\Delta T_f \nabla T_s}(\tau_1, \sigma_1)$$

(21)

$$+ \sum_{\sigma_1=0}^{\mu} L_{Q\Delta T_r^4}(\sigma_1) M_{\Delta T_f \Delta T_r^4}(\tau_1, \sigma_1) + \sum_{\sigma_1=0}^{\mu} L_{Q\Delta T_f}(\sigma_1) M_{\Delta T_f \Delta T_f}(\tau_1, \sigma_1)$$

This representation can be readily extended to the non-linear case.

Facility for the test cell experiment

The experiment consisted of a highly instrumented environmental chamber. The experimental data set used in the present work was collected, from the British Gas plc test cell at Cranfield, by the Energy Monitoring Company (EMC), over the 1989/90 heating season [12].

17

The test cell has internal dimensions of 2.03m by 2.03m by 2.33m tall. The four walls of the test cell, which are of an externally insulated brick construction, are built off an insulated timber floor panel which has been raised on blocks above ground level, allowing the floor panel to be at the ambient external temperature. The flat roof of the test cell is of a timber-frame Styrofoam construction, with waterproofed plywood as the external surface and plasterboard as the internal surface. The internal surfaces of the test cell are finished with a coat of mat white paint.

The test cell is exposed to natural external meteorological conditions. It is highly sealed, as the natural infiltration rate was less than 0.05 ac/hr, as determined from a pressure test on the test cell [12]. The test cell was continuously mechanically ventilated by the outside air, ducted via a pulse output gas meter, to record the ventilation rate, which was set at approximately 2 ac/hr using dampers on the inlet and outlet ducts. This air entered the test cell via a diffuser pipe, running from the floor to the ceiling, in the North-West corner. The air, within the test cell, was heated by a 1 kW convective heater, placed parallel to the North wall, facing into the test cell and controlled by a pseudo random sequence of on/off pulses with a 30 minute time step.

Time series data were collected at 5 minute intervals for a period of 20 days for the experiment. Measurements were obtained for the air and surface temperatures, and for the heat flux flowing into each surface within the test cell. The radiation exchange was determined directly from the net flux measurements and also from the surface temperatures. The convective exchange was determined from the heat flux measurements and from a series of temperature differences measured using a Meyer ladder. A Meyer ladder measures the air temperature through the boundary layer, from the surface to which it is attached to the bulk air, was mounted on the ceiling of the test cell close to the heat flux mat on this surface.

Analysis of environmental chamber data

The use of thick Styrofoam in the construction of the test cell caused the time constant for thermal conduction through the envelope is very long, of the order of days. Hence this path will be assumed to be negligible within the time scale of minutes for either the convective or radiative flow paths considered in this section. The convective and radiative heat transfer coefficients will be determined as the area under the estimated response factor curve for each process. The Meyer ladder also enabled an investigation into the properties of the boundary layer at the ceiling to be performed.

Figures 2, 3 and 4 show typical 24 hour samples for the following variables. In Figure 2, the temperature difference between the tenth sensor on the Meyer ladder and the surface of the ceiling. Figure 3 shows the difference between the surface temperature of the ceiling and the average temperature of the other surfaces within the test cell, both raised to the fourth power, allowing for the Stefan-Boltzmann's constant. (The cubic geometry of the test cell and the fact that all the surfaces within the test cell were finished with a coat of mat white paint mean that the correction due to the relative view factors and the emissivity of each surface will be negligible). Figure 4 shows the heat flux at the ceiling surface, measured as positive into the surface.

The convective and radiative response factors, from which the convective and radiative heat transfer coefficients are determined, were estimated from 5 days (1440 points) of time series data from the data set. The maximum length of time delay or the length of the memory of the processes was set to 3 hours.

Figure 5 shows the convective and radiative heat transfer coefficients or gains. The convective heat transfer coefficient between the ceiling and the bulk air within the test cell is the asymptotic value of the convective HTC curve and is 5.5±0.6 W/m^2 °K. The thickness of the boundary layer at the ceiling in this experiment can be estimated from this curve and is approximately 100mm thick. The radiative heat transfer coefficient is approximately constant, as would be expected, and has a value of approximately 0.5±0.1 W/m^2 °K. This value is a function of the emissivity and absorptivity of the ceiling.

The convective and radiative driving functions for a second data set were used to predict the heat flux at the surface and these predicted valued were then compared with the observed values. Good agreement between the predicted and measured heat flux are clearly seen. Figure 7 shows the predicted convective and radiative components of the heat flux together with the observed heat flux values so that the contribution from each process can be seen.

The above example demonstrates the accuracy and utility of the response factor approach can be appropriately applied to many areas in building performance assessment.

Conclusions

In this work the thermal transport coefficients for a range of different building materials have been determined using the local constitutive and graph network representations. Each of the two representations characterised the measured heat flux well. However, only the local constitutive representation gave consistent and accurate values for the thermal conductivity of the materials examined. The Mitalas and Stephenson directed graph network representation failed to produce consistent or accurate values for the transport coefficients. Thus the Mitalas and Stephenson graph network representation is not likely to provide reliable thermal predictions of buildings performance.

As many of the current calculation procedures are based on this graph network representation it is recommended the further studies be undertaken to develop alternative procedures and extend the experimental studies to cover a wider range of materials, composites and building structures operating in real meteorological conditions.

The moment hierarchy of the local constitutive representation was used to estimate the response factors of the convective and radiative processes, that act at the surface of the ceiling within an tes cell. The response factors provided a good a characterisation of the physical relationship between the physical variables. The area under the estimated response factor is the transport coefficient for that process. The bulk convective and radiative heat transfer coefficients, in this experiment, are 5.5 ± 0.6 W/m^2 °K and 0.5 ± 0.1 W/m^2 °K, respectively. The convective and radiative components of the surface heat flux have also been indicated.

The analyses presented in this work demonstrate the accuracy and utility of the moment hierarchy approach to response factor estimation, and that the local constitutive representation can be appropriately applied to many areas in building performance assessment.

Acknowledgements

References

[1]   Mitalas G P and Stephenson D G, Calculation of Heat Flows Through Walls and Roofs, ASHRAE TRANS., Vol. 74, paper No. 2086, 1968, p 182.

[2]   Mitalas G P and Stephenson D G, Room Thermal Response Factors, ASHRAE TRANS., Vol. 73, paper No. 2108, 1967, p 267.

[3]   Stephenson D G and Mitalas G P, Cooling Load Calculations by the Thermal Response Factor Method, ASHRAE TRANS., Vol. 73, paper No. 2018, 1967.

[4]   ASHRAE research project 515-RP, Dynamic heat transmission characteristics of seven generic wall types, Private Communication.

[5]   Irving A D, Stochastic Sensitivity Analysis, Applied Mathematical Modelling, Vol. 16, January, 1992, p 3.

[6]   Carslaw H S and Jaeger J C, Conduction of heat in solids, Clarendon Press, Oxford, 1959.

[7]   Onsager L, Reciprocal relations in irrervisible processes, I, Phys. Rev., Vol. 37, 1931, p 405.

[8]   Onsager L, Reciprocal relations in irrervisible processes, II, Phys. Rev., Vol. 38, 1931, p 2665.

[9]   Gurtin M E and Pipkin A C, A general theory of heat conduction with finite speed waves, Arch. Ration. Mech. Anal, 31, 1968, p 113.

[10]   Chen P and Nunziato J, Thermodynamic restrictions on the relaxation functions of the theory of heat conduction with finite speed waves, Z. Angew. Math. Phys., 25, 1974, p 791.

[11]   Irving A D, Dewson T and Day B, Time series estimation of the response factors of building components, In CIB W60 report "Some examples of applications of the performance concept in building", Athens, October 1992.

[12]   Martin C and Watson M, Further Experiments in a Highly Instrumented Test Room, Private Communication.

Figure captions
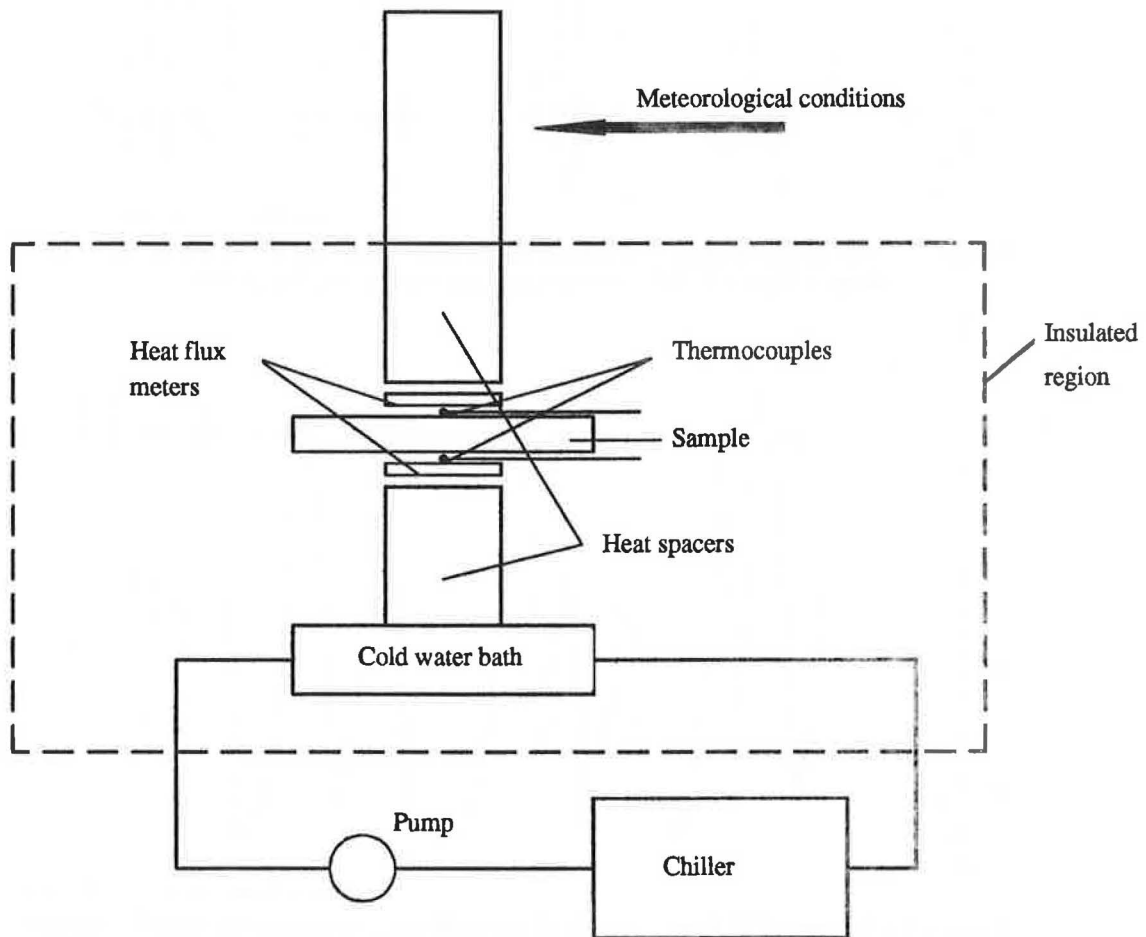
Figure   1. A schematic diagram of the experimental arrangement.
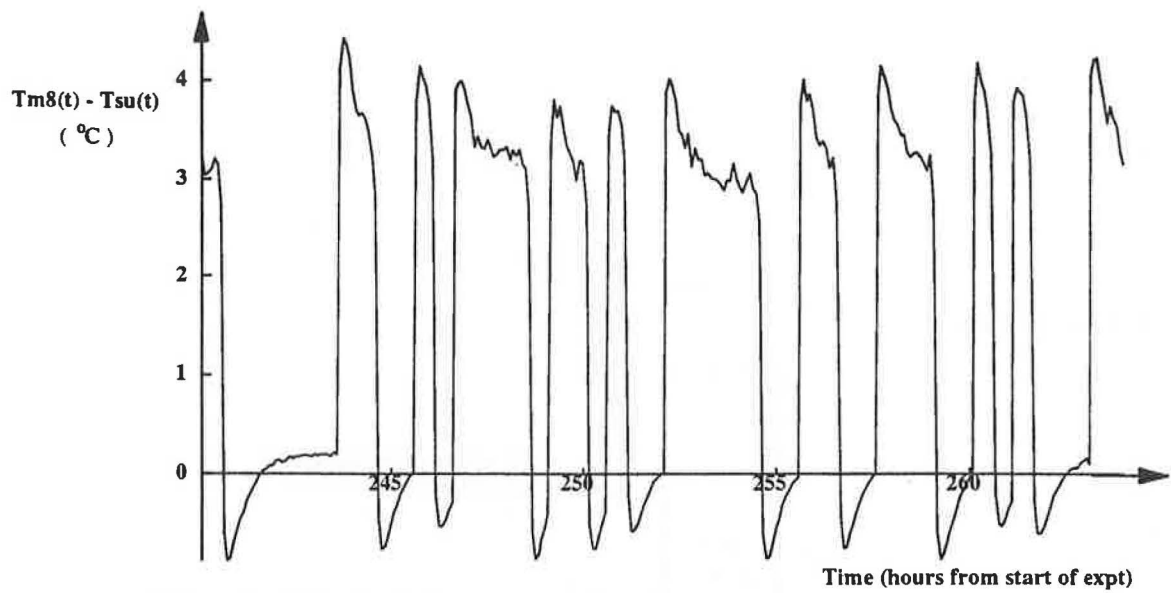
Figure 2 : A typical 24 hour sample of the temperature difference between the eighth Meyer ladder sensor and the surface of the ceiling
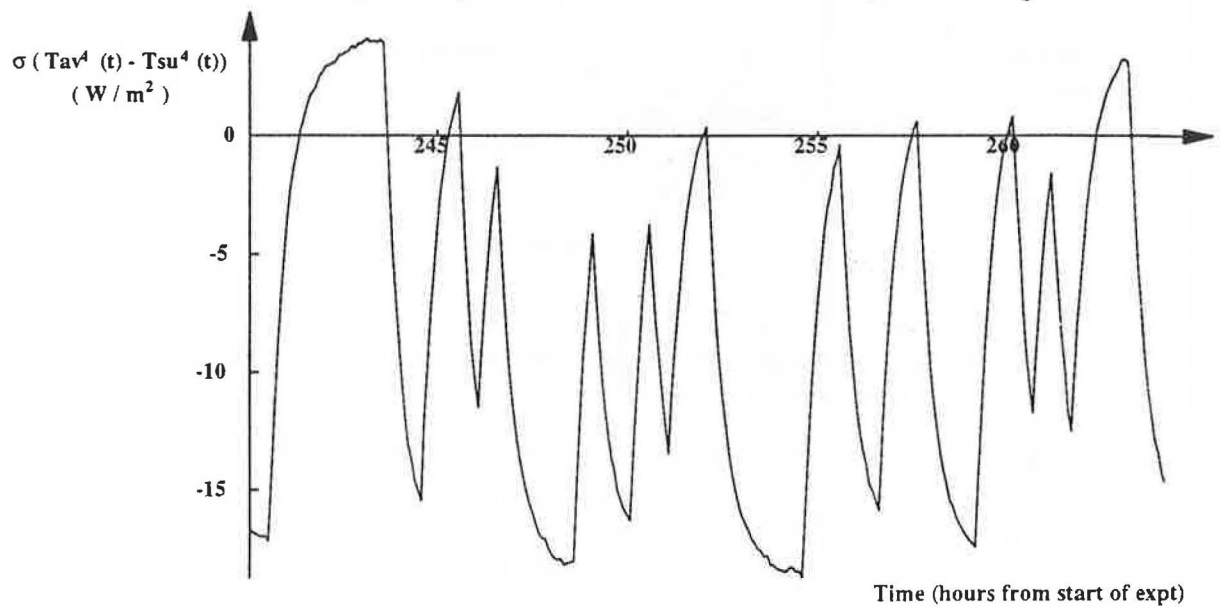

Figure 3 : A typical 24 hour sample of the differnce between the fourth powers of the temperatures of the ceiling surface and average of the remaining surfaces
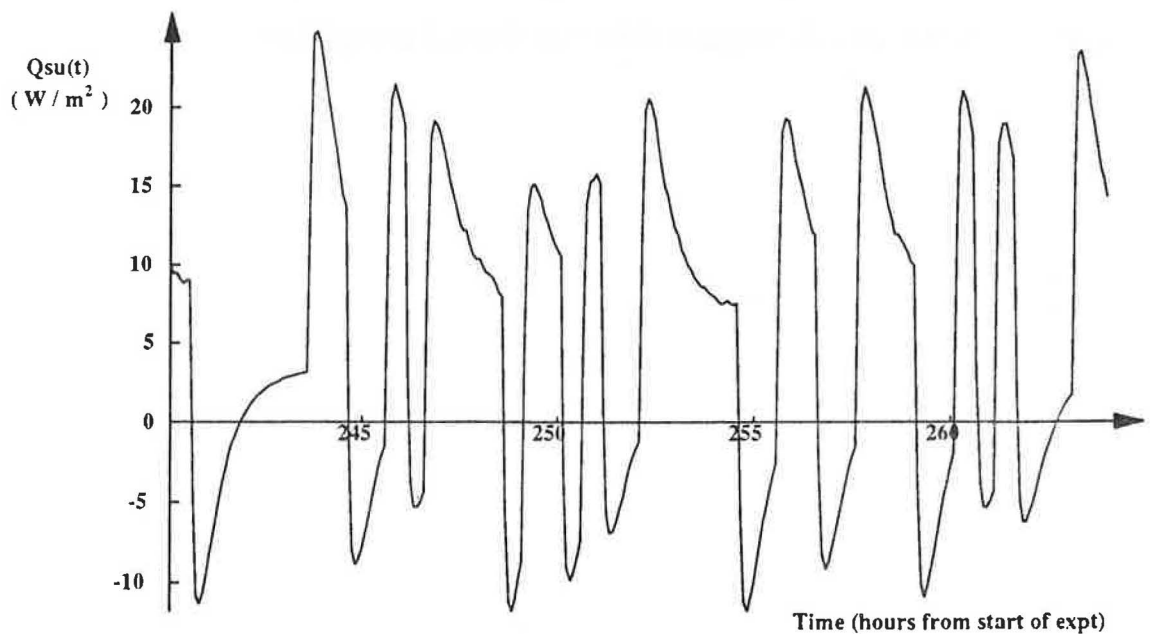

Figure 4 : A typical 24 hour sample of the heat flux at the ceiling surface
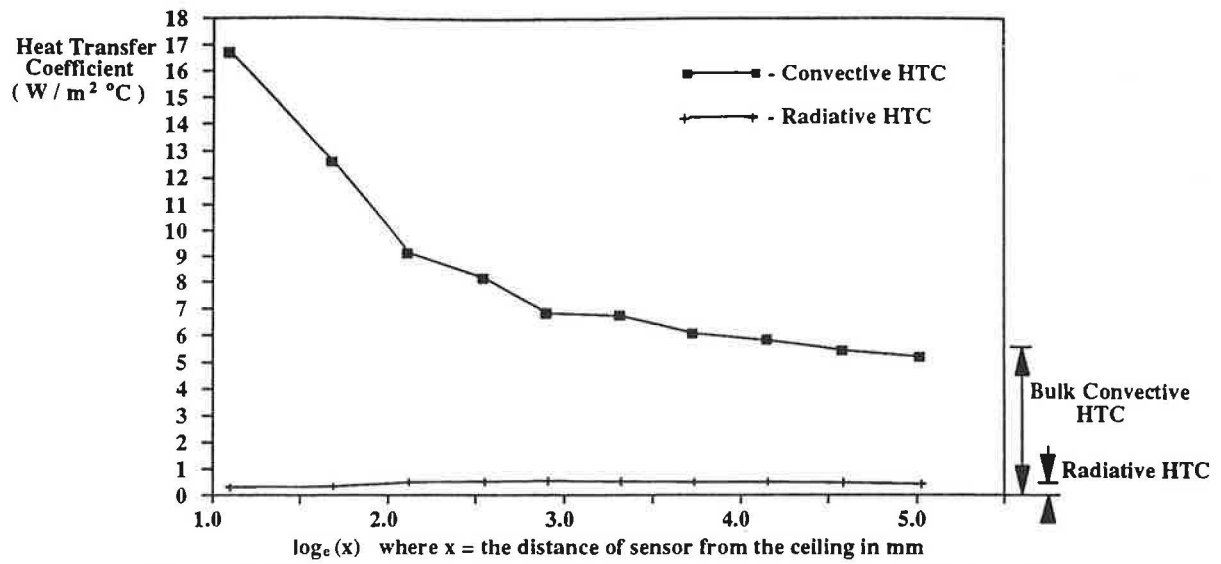
Figure 5 : Estimated convective and radiative heat transfer coefficients for each Meyer ladder sensor, on a natural log scale
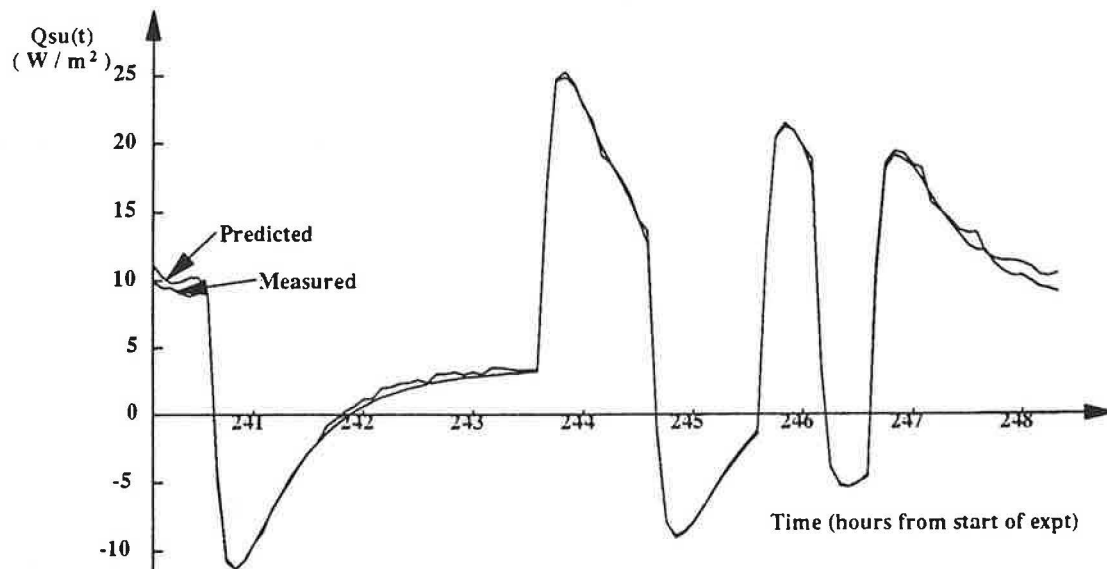

Figure 6 : A sample of the measured and predicted (using the estimated convective and radiative response functions) heat flux at the ceiling surface
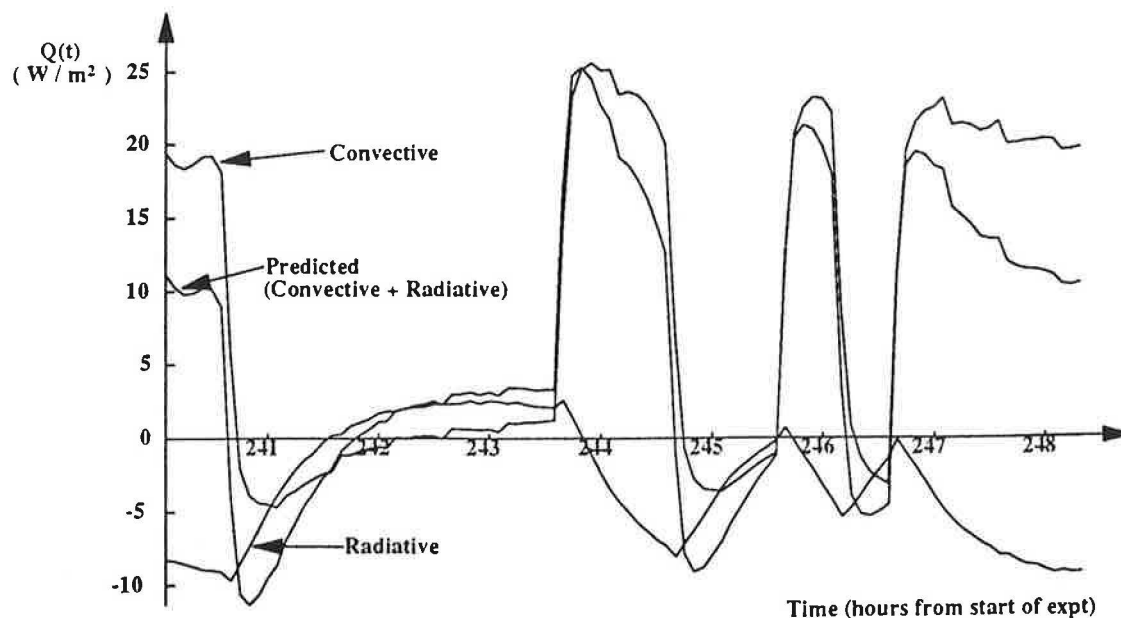

Figure 7 : A sample of the predicted heat flux at the ceiling surface, split into it's radiative and convective components